The fluctuating pressure field in a supersonic turbulent boundary layer

By A. L. KISTLER AND W. S. CHEN†
Yale University

(Received 19 October 1962)

The pressure fluctuations caused by a turbulent boundary layer on a solid surface have been obtained over the Mach number range 1·33–5·00. The root-mean-square values of the pressures are found to be proportional to the local skin friction. The proportionality constant is not a strong function of Mach number in the range investigated but is larger than the previously obtained subsonic values by about a factor of 2. The space-time correlations with the space separation in the direction of the mean flow are characterized by a convection speed U_c, and this speed falls from 0·8 of the free-steam velocity at $M = 1{\cdot}33$ to 0·6 at $M = 5$. The peak value of the correlation coefficient falls to one-half for a spatial separation of the measuring points of about two-tenths of the boundary layer thickness.

1. Introduction

Associated with the irregular motions of a turbulent fluid is a fluctuating pressure field. This pressure field is apparent to the unaided observer through both the sound field associated with the turbulence and the fluctuating force on a solid surface in contact with the turbulence. Recently there has been an increase of interest in the pressures on material surfaces, since when flight vehicles are operated in régimes of large dynamic pressures, these pressures can produce significant effects. The random forces can cause fatigue failure in a structure as well as undesirable levels of structural vibration. In addition, these forces can produce sound within a structure through the intermediate step of forcing the solid surface into motion. There is, consequently, a definite need to obtain information about the turbulent pressure field, particularly for Mach numbers near and above one. With this motivation a programme to obtain measurements of the pressure field on a solid surface adjacent to a supersonic boundary layer was undertaken at the Jet Propulsion Laboratory, where measurements could be obtained over a large Mach-number and Reynolds-number range in the supersonic wind tunnel.

Most of the work done previously on this problem, both theoretical and experimental, has been limited to the study of the incompressible and the low-Mach-number cases. For incompressible flows, the Navier–Stokes equations give a relation between the pressure gradient and certain combinations of velocity derivatives and velocities. The pressure at a point can be computed, therefore,

† Now at A.C. Sparkplug Company, El Segundo, California.

as a line integral of some function of the velocity field. A more tractable approach is to take the divergence of the momentum equations and obtain a scalar expression for the Laplacian of the pressure. This equation is a Poisson equation, where the source terms involve a knowledge of the velocity field; it can be integrated for a particular set of boundary conditions by a Green-function technique, and the solution is at hand if we can make the correct assumption concerning the source terms. Unfortunately, the available experimental results for the turbulent velocity field are not sufficient to support a statement about the source terms free from contentious points; hence the theoretical results do not contain much more information than could be obtained by a simple dimensional argument. Kraichnan (1957) and Lilley & Hodgson (1960) have studied the theoretical problem. Measurements have been made of the wall-pressure fluctuations for subsonic turbulent boundary layers by Willmarth (1959) and Harrison (1958). Their results were used as a guide in setting up these experiments.

There is a definite advantage in going to compressible flows to get information with which to construct a theory, since the ratios of the various derived scales of a shear flow, e.g. the momentum or displacement thickness, can be varied independently by varying the Mach number and Reynolds number. Also, as the Mach number is increased, some phenomena might be accentuated which could help clarify the physical process. It would be desirable to obtain measurements of the pressure field throughout the turbulence in order to construct a rational theory. Unfortunately, measurements anywhere except at the wall represent an almost impossible problem since any pressure-sensitive device in the flow responds both to static pressure and local velocity fluctuations.

2. Aerodynamic equipment

The measured flow fields were produced in the JPL 20 in. supersonic wind tunnel. This continuous flow tunnel has a flexible plate nozzle which permits Mach numbers up to 5·0 to be attained. The top and bottom surfaces of the 18×20 in. cross-section working area are made up of flexible plates whereas the side-walls are plane upstream of the throat through the working section. The nozzle produces a uniform flow in the working section to within $\pm 1\%$ of the Mach number, M, over its whole range. The settling chamber contains an array of screens to act as turbulence reducers, and measurements have shown that the turbulence in the main stream of the working section is almost wholly caused by sound radiated from the turbulent boundary layers on the tunnel walls (Laufer 1961), which is the irreducible minimum unless these boundary layers can be removed.

The specific flow fields investigated were the boundary layers on a flat plate mounted in the tunnel and the boundary layers on the flat side-wall of the working section. The mean properties of these boundary layers closely approximated the properties of equilibrium, adiabatic, flat-plate boundary layers; therefore, the boundary layers are assumed to be uniquely characterized by the free-stream Mach number and by a Reynolds number based on some thickness.

The air supply of the tunnel was dried sufficiently to prevent water condensation. The tunnel stagnation temperature was approximately 100° F; stagnation pressure ranged from about 20 to 300 cm Hg.

The flat plate used for these tests was 1 in. thick, 18 in. wide, and 33 in. long. It spanned the tunnel along the horizontal mid-plane of the working section. The plate was flat on the surface upon which the measurements were taken, the opposite surface being bevelled at 24° at the upstream end to form a sharp leading edge. The leading edge was perpendicular to the stream direction with a radius of curvature of a few thousandths of an inch. A row of small holes through which air could be blown to effect the transition of the boundary layer was located near the leading edge of the test surface. The plate installed in the tunnel is shown in figure 1 (plate 1).

The major problem in measuring the pressure fluctuations is the isolation of the pressure pick-up from the accelerations associated with the vibration of the tunnel. Because of variations in tunnels, flow fields, and transducers, there is no general solution for this problem. In these tests it was found sufficient to support the flat plate in the tunnel with four bolts extending through the side walls in rubber bushings. This mounting scheme together with a suitable transducer, described in § 3, resulted in an output due to pressure significantly larger than that from acceleration for a substantial range of flow conditions. In order to obtain measurements of the pressure fluctuations on the side-wall, it was found necessary to mount the transducer on a disk that could be inserted into a hole in the side-wall with its surface flush with the surface of the side-wall (figure 2, plate 2). The disk had to be supported at another point in the tunnel structure where vibrations were at a minimum. The area around the disk was sealed with rubber.

The flat-plate configuration was used in the early stages of these experiments and had the advantage that both a laminar and a turbulent boundary layer could be produced over the transducer for the same tunnel conditions. Also, a large variation in the boundary-layer Reynolds number at the transducer site could be obtained by varying both the tunnel pressure and the transducer location. The size and frequency requirements for quantitative measurements on the plate were so extreme, however, that as soon as the side-wall mounting problem was solved, most of the data were obtained there. The size and frequency requirements were eased by a factor of about five compared to the plate.

3. The pressure transducer

The three major requirements for a pressure transducer are that it have a sufficiently large frequency range, that it be sensitive enough so that the output is larger than the electrical noise of the associated equipment, and that it be small enough to approximate a point compared to the relevant scales of the pressure field.

It is known that the spectrum of the velocity fluctuations in a supersonic turbulent boundary layer shows significant energy out to a frequency range of about $5U_\infty/\delta$, where U_∞ is the free-stream velocity and δ is the geometrical boundary-layer thickness—the distance from the wall at which the mean velocity in the boundary layer becomes equal to the free-stream velocity. With the stagnation temperature that was used, the free-stream velocity was of the order of 2000 ft./sec. On the plate, δ ranged from 0·1 to 0·4 in.; on the side-wall, it varied

from 1 to 2 in. Therefore, assuming the pressure scales were comparable to the velocity scales, the response of a transducer has to extend to 600 kc/s on the plate and to 150 kc/s on the side-wall. The side of the transducer should be smaller than $0{\cdot}2\delta$ or ideally smaller than 0·02 in. on the plate. The transducer (figure 3 and figure 4, plate 3) developed for use within these limits used a small

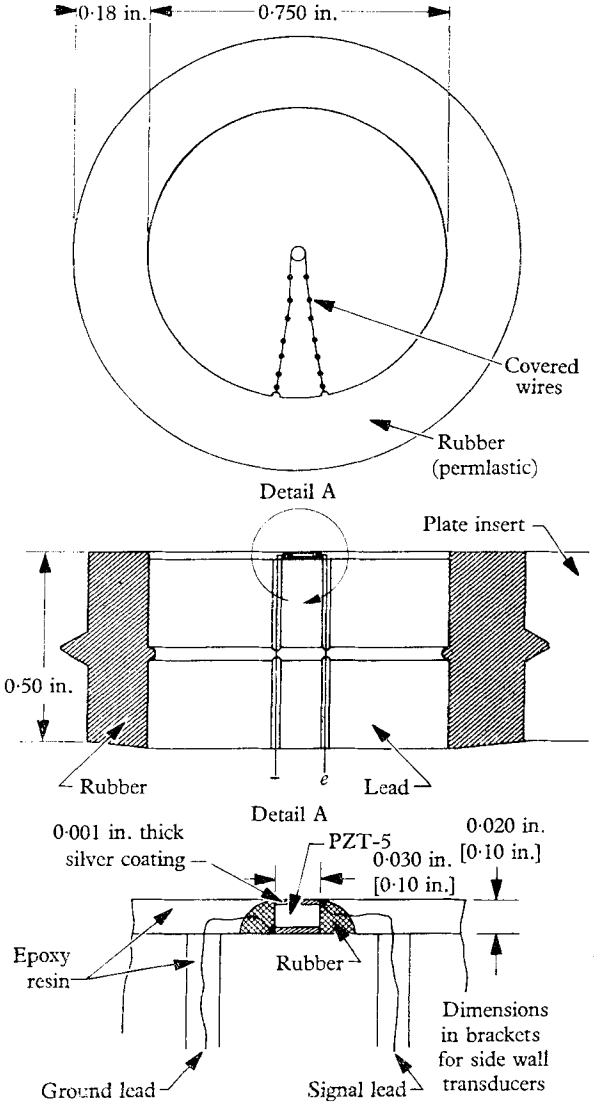

FIGURE 3. Drawing of pressure transducer.

lead zirconate element† as the electromechanical transducer. This particular configuration is the result of long development and yielded meaningful pressure measurements for the particular set of conditions encountered. The design features of the particular mounting are as follows:

(1) The surface of the pressure-sensitive element is flush with the wall; there

† PZT-5, manufactured by the Clevite Corp., Cleveland, Ohio.

are no open spaces on the surface. It was found that leaving an air gap (of approximately 0·002 in.) around the element in order to isolate it from vibration resulted in a strong extraneous output whose frequency corresponded to that of a Helmholtz resonator of the volume and area present. This frequency fell within the range of interest, i.e. less than 600 kc/s, and the air gap was eliminated.

(2) Only a single piece of PZT-5 was used. All attempts at making a layered structure, either to increase the sensitivity or to cancel some accelerations, resulted in extraneous signals in the frequency range of interest (1–600 kc/s). The material used was either a cut-down piece of PZT-5 disk, or, for thin pieces (0·020 in. thick) a piece of the PZT-5 element of a Clevite TF-01A electromechanical transformer. PZT-5 has one of the highest Curie points of any commercially available piezoelectric ceramics, so that the leads could be soldered directly to the silver layer on each face.

(3) The major resonant frequency of the transducer is determined by the thickness of the piezoelectric material, and can be increased to well above 600 kc/s by using material of sufficiently small thickness (0·02 in.).

(4) The physical area in contact with the flow can be reduced to a circle 0·015 in. in diameter. Transducers with sensitive elements of various sizes were produced, with thicknesses ranging from 0·02 to 0·1 in. and diameters ranging from 0·015 to 0·1 in.

(5) Any motion of the leads from the piezoelectric element can produce a spurious output signal if the leads are near a conducting surface (capacity change). These leads were imbedded in epoxy resin and held rigidly until they could be brought away from the structural surface.

(6) In order to get sufficient isolation of the transducer from the vibration of the plate or wall disk, it was mounted in rubber. The vibrations of the transducer on this support gave the low-frequency limit to the measurements, and in order to make this frequency as low as possible, a lead cylinder was used to back up the ceramic element. The size of this cylinder was controlled by the available clearance space.

When the transducer is considered as a unit, the following remarks can be made. The stresses in the sensitive element that are interpreted as a pressure signal on the exposed surface can actually come also from pressures exerted on the epoxy surface and transmitted through the lead or rubber. That this energy was small compared to the direct action of the pressure on the ceramic element was shown by transducers in which the epoxy resin had been hollowed out. Only the epoxy surface and edge were left; consequently, the lead backing was somewhat decoupled from the surface. In test situations, the outputs of these transducers were no different from outputs of transducers with solid epoxy build-ups. The possibility that an intense standing wave pattern existed in the backing block was also checked by using different backing materials (glass and steel) and by modifying the shape of the backing block (grooving). No effect was observed with any of these modifications. For some reason no measurement showed a frequency that could be attributed to acoustic waves in the backing block. The strongest vibration associated with the transducer itself was the low-frequency resonance of the lead backing on its rubber support, which occurred

at around 500 c/s. Of course, a particular transducer might show unexplained signals at any frequency, but these could be attributed to construction variations; particularly bad transducers were simply not used. Since it was found that the larger transducers could be made with more stable characteristics, these were used exclusively on the side-wall where the boundary layer was of sufficient thickness.

An attempt was made to clarify a phenomenon pointed out by Willmarth (1958). In calibrating his transducers, which were similar to those described here, he found that the electrical capacity between the ceramic and the backing could change when a pressure was applied to the sensitive surface, and that this could produce an undesirable component in the output of the transducer. By using a double element with both exposed faces grounded, he seemingly avoided this problem. Double elements could not be used here, so that this effect was subjected to some investigation. The tests on the transducers showed no significant capacity-change effect, but did turn up a pyroelectric effect. A temperature variation on the surface, such as might be produced by a shock wave passing over the transducer, did produce an output voltage. The response time for this pyroelectric effect is controlled by the silver layer on the surface, and, for the elements used here, was about 1 msec. The spectral region below 1 kc/s already had a strong contribution from the transducer vibrating on its mount, so that all the frequencies below 1 kc/s were filtered out, and this effectively eliminated the temperature signal from the output.

In order to estimate the frequency and phase response of the transducers to the imposed pressure, it is necessary to set up some model of the mechanical system. The pressure input can be assumed to come from a zero-impedance source; i.e. the motion of the transducer face should not affect the pressure input. The experimental results related in the preceding paragraph can be interpreted as showing that the backing can be taken as a semi-infinite field, so that no standing waves have to be accounted for. This model corresponds to the classical problem of an organ pipe, forced at one end and radiating at the other. The model is defective inasmuch as the backing material is also forced in the neighbourhood of the piezoelectric element by the pressure field. The analysis showed that for the material constants encountered here the design should give an essentially uniform response, as measured by the ratio of strain to pressure for the frequency range in which they were used, i.e. up to 600 kc/s for the 0·030 in. diameter, 0·02 in. thick elements. In order to calibrate the transducers, they were located on the side-wall of a shock tube and a shock wave was passed over them. Shock strength was determined by measuring the shock speed and temperature. The output signal was recorded by an oscilloscope. The response of the transducers to the shock wave was a sharp rise (determined mainly by the transit time of the shock over the sensitive element) and a slow oscillation at about 500 c/s due to the mounting. A typical calibration trace, for a transducer with a 0·1 in. diameter and a 0·1 in. thick PZT-5 element, is shown in figure 5. Another check on the response characteristics of the transducers was obtained by blowing a small high-speed jet of air over their surfaces. Such a jet is a convenient source of an effectively continuous spectrum of high-frequency pressure fluctuations, and any defects in construction showed up as spikes in the response spectra.

The sensitivity of the transducers ranged from 20 to 100 mV/p.s.i., depending on size as well as variations in construction. Some transducers were constructed with two or more tandem elements on the surface so that space-time correlations with a small spatial separation could be obtained. In so far as could be determined, these elements were electrically and mechanically separate.

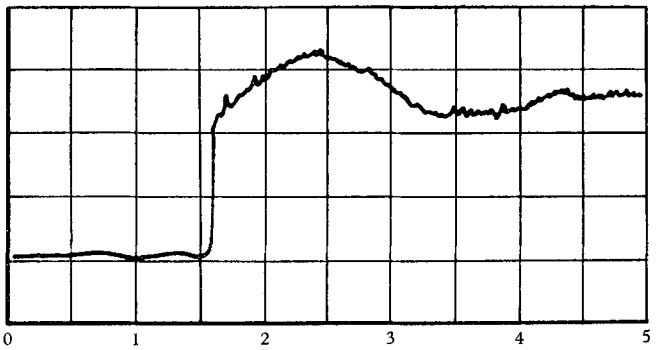

FIGURE 5. Shock-tube response transducer, arbitrary units.

4. Electrical equipment

A strain of a piezoelectric material produces a surface charge which is distributed between the capacity of the element and any capacity in parallel with it. The charge decays with a time constant determined by the total capacity and the resistance shunting the element. In order to maximize the voltage across the element, it is therefore essential to minimize the shunt capacity, and in order to get good low-frequency response, the shunt resistance should be as large as possible.

The large resistance is obtained by using a cathode follower as the input stage of the voltage amplifier. The one used here was of conventional design with an input resistance of about 100 MΩ. The cathode follower circuit included a high-pass filter with a variable low-frequency cut-off which could be set between 0 and 10 kc/s. The shunt capacity consists primarily of the lead capacity between the transducer and the cathode follower. It can be minimized by locating the cathode follower as close to the transducer as possible. An attempt to build a cathode follower that could be mounted inside the flat plate next to the transducer was unsuccessful because the tube microphonics in this noisy environment dominated the signal. It is not possible to build a solid-state circuit with sufficiently large input resistance for this purpose. The cathode follower was therefore located outside the tunnel, requiring about 18 in. of coaxial cable between the transducer and the amplifier.

When shaken, cables produce electrical noise, probably from the strands of the shield rubbing together. Commercially available low-noise Microdot cable (shield impregnated with graphite) with a capacity of 1 $\mu\mu$F/in. was used. The transducer capacity was normally about 15 $\mu\mu$F, so that a substantial fraction of the signal was lost in the cable. This loss can be decreased by driving the cable shield with the cathode follower to the voltage of the transducer; but this seemed to add more noise to the signal, and a passive cable was used in these tests.

The output of the cathode follower went to a wide-band, low-noise voltage amplifier; the output of the amplifier went to various instruments—wave analysers, mean-square voltmeters, etc., depending on the measurement to be made. A detailed description of the instrumentation is given by Chen (1961).

The only specialized electronic instrumentation developed for these tests was a digital correlator. In order to measure the space-time correlation of the pressure signals on a surface, it is necessary to obtain the mean product of the output voltages of two transducers, where the product is formed from the output of one transducer at a given time and the output of the other at a fixed time-interval later. To perform this operation, the first technique tried was to delay one signal by a lumped-circuit delay line and multiply the signals by a quarter-square technique. All the correlations obtained on the flat plate were measured in this fashion. This techique is limited in band-width since the band-width of a lumped circuit delay line is inversely proportional to the delay time increment. For large band-widths, many small steps are required, and then the attenuation per step affects the output. The delay line used had 1 μsec steps and an effective band-width of about 100 kc/s. This band-width was certainly not adequate to give convincing results for the plate or for the side-wall boundary-layer measurements. A digital correlator was developed that had a useful band-width of 200 kc/s and a more accurate time delay mechanism. The digital correlator was completed at about the same time as the side-wall mounting problem was solved so that it was used for all the side-wall measurements. One operation of this correlator can be described as follows: At time zero, one signal is sampled and its value converted to a digit between -7 and $+7$ by a gate circuit. This number is stored. At time τ later, the other signal is converted to a digit between -7 and $+7$. This number and the stored digit are multiplied. The entire operation could be repeated up to 5000 times per second, and the number of operations as well as the sum of the products was recorded after a convenient time interval, usually about 1 min. The mean product was then computed. The delay time τ could be varied continuously from 0·01 μsec to 10 sec. The correlator is described in a paper by J. Stallkamp which is to be published soon.

5. Measurement errors

In order to describe the statistical properties of the pressure fluctuations at the wall, two types of data were obtained: the temporal power spectra at a given point, and the space-time correlation between two points. The main sources of error in these data are the contamination of the signal with the radiated pressure field from the tunnel walls and the effect of the finite area of the transducer.

The relative magnitude of the direct, local pressure fluctuation and the radiated pressure could be measured on the flat plate. When the natural transition of the boundary layer on the plate surface was downstream of the transducer, a direct measure of the radiated pressure was obtained. If transition was moved upstream of the transducer by using the air trip but keeping the tunnel conditions fixed, the local pressure fluctuations were obtained. A set of these measurements is shown in figure 6. The radiated pressure is seen to be an insignificant contribution to the total signal. It was not possible to perform a similar

experiment on the tunnel side-wall, but it is assumed that the same result would have been obtained. It should be noted that the two cases are not directly comparable since, for the flat plate, the radiation originates in the tunnel boundary layers, which are of significantly larger scale than the boundary layer on the plate; whereas for measurements on the side-wall, the radiating boundary layers and the measured boundary layer are of comparable scale. Laufer's measurements of the radiation field, however, show the sound pressure level to be significantly smaller than the direct pressure level.

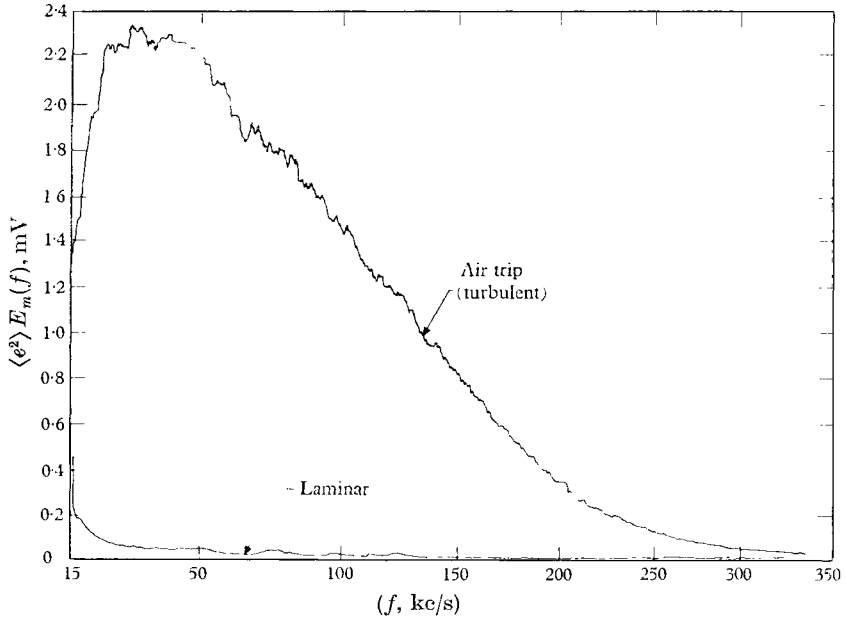

FIGURE 6. Transducer output spectra for radiated and local boundary-pressure fluctuations. $M_\infty = 2{\cdot}21$, $\bar{p} = 190$ mm Hg, $\bar{T} = 56$ °F; cathode-follower filter = 10 kc/s.

The problem of the effect of the finite size of transducers on the measured spectra and correlations can be attacked experimentally by making measurements with a variety of transducers of different size and then extrapolating the results to zero transducer size. In order to apply this method, it is necessary to be able to make measurements with transducers approaching a point in size compared to the pressure scales, or the extrapolation will be subject to much uncertainty. An alternative approach was used here. Corcos, Cuthbert & von Winkle (1959) have treated the length-correction problem and, analytically, have shown that with a set of assumptions that are consistent with the known experimental findings a usable length-correction technique can be obtained. Their results, with some modifications, were used here.

The space-time correlation function for the pressure fluctuations is defined as

$$\langle p^2 \rangle R(\Delta x, \Delta y, \tau) = \langle p(x, y, t)\, p(x + \Delta x, y + \Delta y, t + \tau) \rangle,$$

where $\langle\ \rangle$ denotes a time average, p is the fluctuating component of the pressure at the wall, and x and y are Cartesian co-ordinates in the plane of the plate, x

being aligned with the flow. It is assumed that the pressure field is sufficiently homogeneous in the (x, y)-plane for the variation of $R(\Delta x, \Delta y, \tau)$, the correlation coefficient, with x and y to be neglected compared to its variation with Δx, Δy, the separations of the two transducers in the two co-ordinate directions, and τ, the time increment.

If we measure the output voltage e at a point with a transducer of sensitivity s V/p.s.i. in.^{2}, the measured mean-square voltage is given by

$$\langle e^2 \rangle = s^2 \langle p^2 \rangle \iiiint R(x-\xi, y-\eta, 0)\, dx\, dy\, d\xi\, d\eta,$$

where the integration is over the surface of the transducer in both sets of variables x, y and ξ, η. Consequently, in order to find $\langle p^2 \rangle$ from $\langle e^2 \rangle$ we need the correlation function of the pressure. The power spectrum of e and the space-time correlation of e are most easily accessible to measurement. Therefore, we would like an estimate of the integral above that is obtainable from the properties of these quantities. The two assumptions that give this estimate from the measured quantities are:

(1) The correlation function is a function of $(x-\xi)$ and τ only through the combination $x-\xi-U_c\tau$, where U_c is a parameter, the convection speed, determined by experiment. This assumption permits one to obtain the x variation of the correlations (spectra) from the measured time spectra. When we later discuss the measured correlation functions of e, the justification and limitations of this assumption become apparent.

(2) The correlation function is separable in the (x, y)-plane; i.e. $R(x-\xi, y-\eta, 0)$ is equal to $Q(x-\xi)\, G(y-\eta)$, and, in particular, we will assume that $Q(x-\xi)$ is the same function as $G(y-\eta)$. This assumption is made in order to get explicit results and is not contradicted by available experimental information. Some low-speed measurements by Corcos of the correlation $G(y-\eta)$ indicate that the correlation function R has essentially the same scale in the x- and y-directions.

If we apply these assumptions to a transducer with a square sensitive area of side length $2L$, we obtain the result

$$\langle p^2 \rangle = \frac{\langle e^2 \rangle}{s^2 A^2} \left[\int_0^\infty \frac{E_m(\omega)\, (\omega L/U_c)^2}{\sin^2 (\omega L/U_c)}\, d\omega \right]^2,$$

where $\omega = 2\pi \times$ (frequency), $E_m(\omega)$ is the measured power spectrum of the voltage and is scaled such that $\int_0^\infty E_m(\omega)\, d\omega = 1$, and A is the sensitive area, $4L^2$. Within the same framework of assumptions, the true shape of the time spectrum of the pressure fluctuations at a point can be obtained by dividing the measured spectrum of e at each frequency by the function

$$\sin^2 (\omega L/U_c)/(\omega L/U_c)^2.$$

The results for a round sensitive area are similar to these results if $E_m(\omega)$ falls to small values for $(\omega L/U_c) < 1$. With the approximation

$$\frac{J_1^2\{(\omega r/U_c)^2 + (rK_2)^2\}^{\frac{1}{2}}}{(\omega r/U_c)^2 + (rK_2)^2} \approx \frac{J_1^2(\omega r/U_c)}{(\omega r/U_c)^2} \frac{J_1^2(rK_2)}{(rK_2)^2}$$

for $(\omega r/U_c)$, $rK_2 \ll 1$, and where J_1 is the Bessel function of the first kind, r is the sensitive area radius, and K_2 is the fluctuation wave-number in the y-direction, one obtains

$$\langle p^2 \rangle = \frac{\langle e^2 \rangle}{s^2 A^2} \left[\int_0^\infty \frac{E_m(\omega)\,(\omega r/U_c)^2}{J_1^2(\omega r/U_c)}\, d\omega \right]^2.$$

The sensitive area of the transducer was nominally round so that the correction formula using the Bessel-function kernel was used in reducing the data. The shape and size of the sensitive area are not necessarily the same as the shape and size of the ceramic element, since the mechanical working of the element affects the distribution of polarization. A typical example of how the correction proceeds is shown in figure 7. The measured spectrum is first divided by $J_1^2(\omega r/U_c)/(\omega r/U_c)^2$,

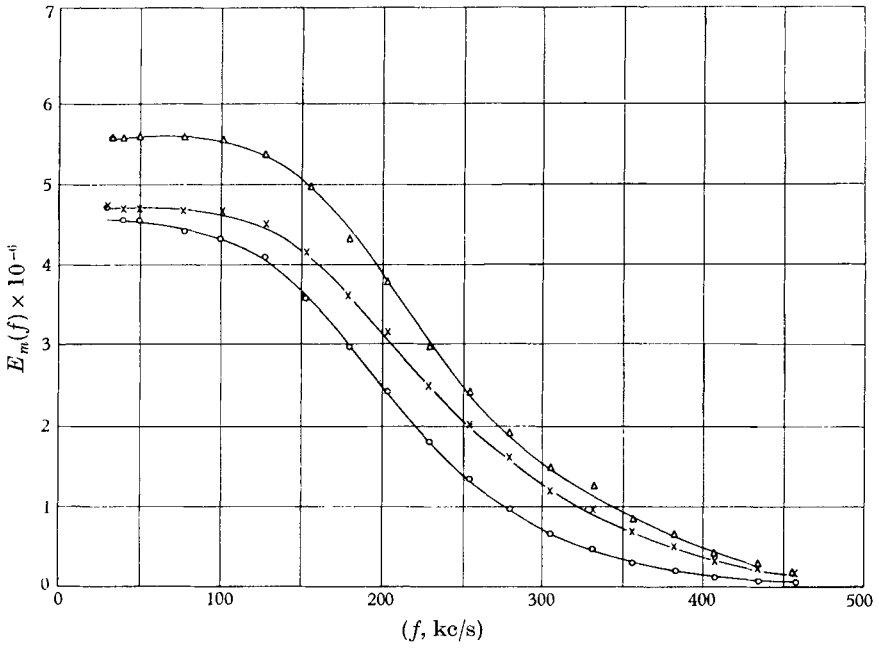

FIGURE 7. Example of the length correction applied to the measured voltage spectrum. $M = 3{\cdot}62$, d (transducer diameter) $= 0{\cdot}030$ in., $\delta^* = 0{\cdot}09$ in., $U_\infty = 2{\cdot}50 \times 10^4$ in./sec, $U_c/U_\infty = 0{\cdot}75$ for this calculation; ○, $E_m(f)$, normalized to $\int_0^\infty E_m(f)\,df = 1$; ×, $E_1(f) = E_m(f)\,(\pi fd/U_c)^2/J_1^2(\pi fd/U_c)$; △, $E_1(f) \int_0^\infty E_1(f)\,df$.

where U_c is obtained from the measured correlation function. This gives a first approximation to the true shape of the spectrum of the pressure at the measuring point. Then the level is changed by the ratio of the spectrum area before correction and after correction. The area under this new curve is then the correct area for determining $\langle p^2 \rangle$; $\langle e^2 \rangle$ is obtained by integrating the measured spectrum $\langle e^2 \rangle E_m(\omega)$. This correction procedure gives a first approximation to the true pressure amplitude at a point but a somewhat rough approximation to the shape of the true time spectrum. Therefore, only those spectral shapes are shown in this report where the correction was not large, and for the most part they are shown uncorrected. As a final remark, it should be mentioned that in those few

cases where sufficient data were available to find $\langle p^2 \rangle$ from several measurements of $\langle e^2 \rangle$ obtained with transducers with sensitive areas of different sizes, the correction procedure outlined above gave about the same value for $\langle p^2 \rangle$.

6. Measurements

Spectra

The area-normalized power spectra of the pressure fluctuations are shown in figure 8. Most of these data were obtained on the tunnel side-wall. The frequency co-ordinate used is $f\delta/U_\infty$, where δ is the geometrical boundary-layer thickness, f is the measured frequency, and U_∞ is the free-stream velocity. In this particular

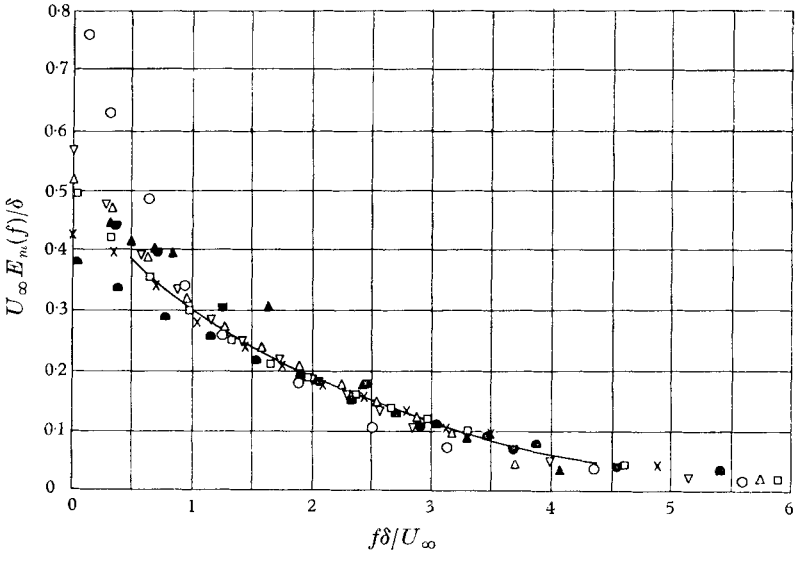

FIGURE 8. Spectra of the pressure fluctuations.

	M	$Re_\theta \times 10^{-4}$	$U_\infty/\delta \times 10^{-3}$ (sec^{-1})	δ(in.)	δ/r	
○	1·33	3·50	16·1	0·99	19·8	Side-wall data, no length correction
△	2·01	1·57	16·3	1·25	25·0	
▽	2·60	1·51	17·5	1·35	27·0	
□	3·50	1·55	15·2	1·70	34·0	
×	3·99	1·65	13·9	1·95	39·0	
●	4·54	1·47	12·6	2·20	44·0	
▲	2·01	0·176	74·0	0·275	18·3	Flat plate data, length correction
◒	4·76	0·414	61·0	0·47	31·4	

co-ordinate system it is apparent that, for decreasing Mach numbers, more energy becomes concentrated at smaller non-dimensional frequencies. The side-wall data shown are not corrected for the finite transducer size. If we assume that the data give the true shape of the pressure spectra, then an estimate can be obtained of the maximum transducer size that will yield reasonable values for $\langle p^2 \rangle$ without correction. The correction should be small for $f\delta/U_\infty \leqslant 5$ on the basis of the given data. The length correction depends on the parameter

$2\pi fr/U_c$, and if corrections to the spectral shape should be less than 25 % then $2\pi fr/U_c$ should be less than 1. If

$$f\delta/U_\infty = 5 \quad \text{and} \quad 2\pi fr/U_c = 1 \quad \text{then} \quad r/\delta \approx (U_c/U_\infty)/10\pi = 0{\cdot}6/10\pi \approx \tfrac{1}{50},$$

where 0·6 is a measured value of U_c/U_∞. Therefore, r/δ should be less than $\frac{1}{50}$. For the side-wall boundary layer, $r/\delta \approx \frac{1}{40}$ at $M = 4{\cdot}7$ and $r/\delta \approx \frac{1}{20}$ at $M = 1{\cdot}33$. Consequently, the size effect is not particularly small for the low-Mach-number cases. Owing to the tentative nature of the length correction, however, the data are shown uncorrected. With the transducer sizes used, it is not possible to obtain meaningful spectral data for large frequencies, i.e. $f\delta/U_\infty > 5$ or get the Reynolds number effect on the spectral shapes for these frequencies. Some corrected flat plate measurements are included in the figure to show that the spectral shapes are roughly the same as for the wall measurements.

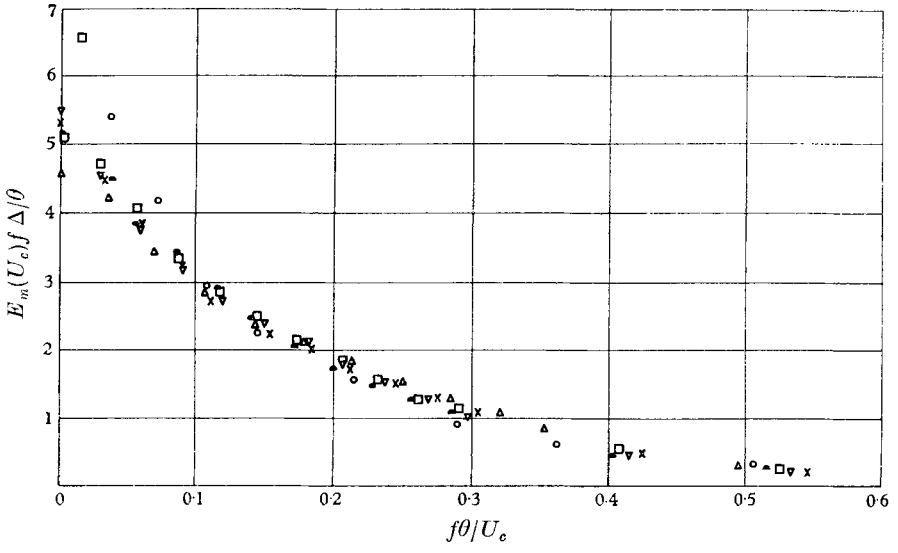

FIGURE 9. Spectra of the pressure fluctuations using θ and U_c to non-dimensionalize the co-ordinates. ○, $M = 1{\cdot}33$; △, $M = 2{\cdot}01$; ▽, $M = 2{\cdot}60$; ×, $M = 3{\cdot}50$; □, $M = 3{\cdot}99$; ●, $M = 4{\cdot}54$.

If we assume that the pressure field is convected past the transducer as a frozen pattern with a velocity U_c (the evidence for this assumption is covered in the following section) then it is possible to relate the measured frequency to the spatial scales of the fluctuation field. In particular, the integral scale of the pressure correlation $R(\Delta x, 0, 0)$, defined as $L_p = \int R(\Delta x, 0, 0)\, d(\Delta x)$ is simply related to the intercept of the pressure spectrum on the $f = 0$ axis. For the co-ordinate used, i.e. $f\delta/U_\infty$, the result is $L_p/\delta = (U_c/4U_\infty)/[U_\infty E_m(0)/\delta]$. The values for this ratio range from 0·16 at $M = 1{\cdot}33$ to 0·057 at $M = 4{\cdot}54$. Since this variation is approximately the same as the variation in the ratio of the boundary-layer momentum thickness θ to the geometrical thickness, the spectra are plotted in figure 9 using the frequency co-ordinate $f\theta/U_c$. This method of plotting brings all the data except those at $M = 1{\cdot}33$ into approximate coincidence. Since the

effect of the finite transducer size is to increase the apparent scale, the $M = 1{\cdot}33$ data, where this error is the largest, might be showing this effect. However, the $M = 2{\cdot}00$ data would have about the same length correction and the scale is significantly smaller than at $M = 1{\cdot}33$. The conclusion is, therefore, that the relative scale does increase for Mach numbers less than 2. A measurement by

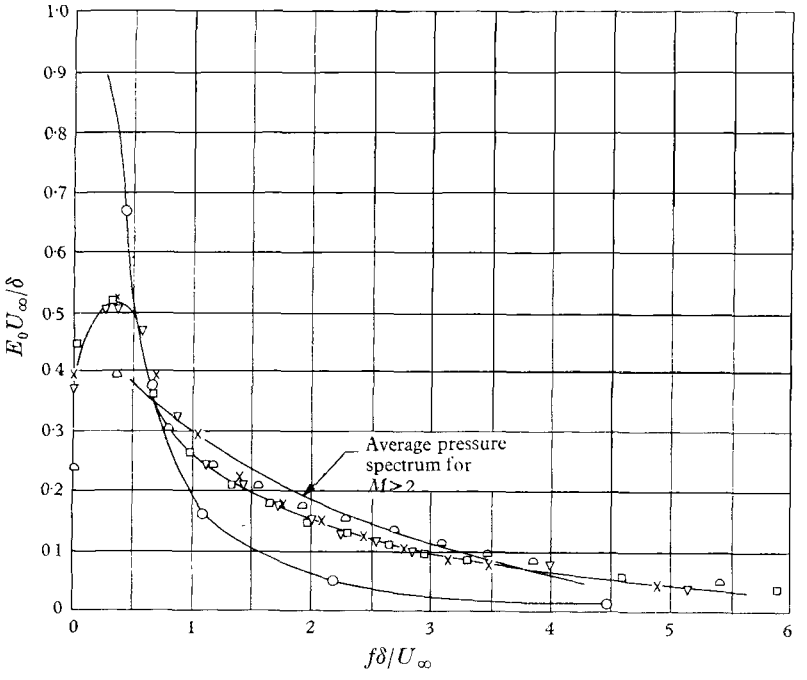

FIGURE 10. Spectra of a hot-wire signal near the centre of the boundary layer.

	M	$Re_\theta \times 10^{-4}$	$U_\infty/\delta \times 10^{-3}$ (sec^{-1})	δ(in.)	z/δ	
▽	2·60	1·51	17·5	1·35	0·50	Side-wall data
□	3·50	1·55	15·2	1·70	0·50	
×	3·99	1·65	13·9	1·95	0·50	
⌓	4·54	1·47	12·6	2·70	0·50	
○	0·045	1·0	0·20	3·00	0·58	Klebanoff (NACA TN 3178)

FIGURE 11. Measured space-time correlations on the tunnel side-wall. △, $\Delta x = 0{\cdot}25$ in., ○, $\Delta x = 0{\cdot}50$ in., $d = 0{\cdot}10$ in.

	M	U_∞ (in./sec)	Re_∞	δ (in.)
(*a*)	2·01	20,400	$1{\cdot}95 \times 10^4$	1·10
(*b*)	3·99	25,800	$3{\cdot}4 \times 10^4$	1·78
(*c*)	5·00	27,800	$2{\cdot}22 \times 10^4$	2·05
(*d*)	1·33	15,900	$3{\cdot}5 \times 10^4$	0·99
(*e*)	3·01	24,500	$1{\cdot}39 \times 10^4$	1·35
(*f*)	4·54	27,100	$3{\cdot}25 \times 10^4$	1·90

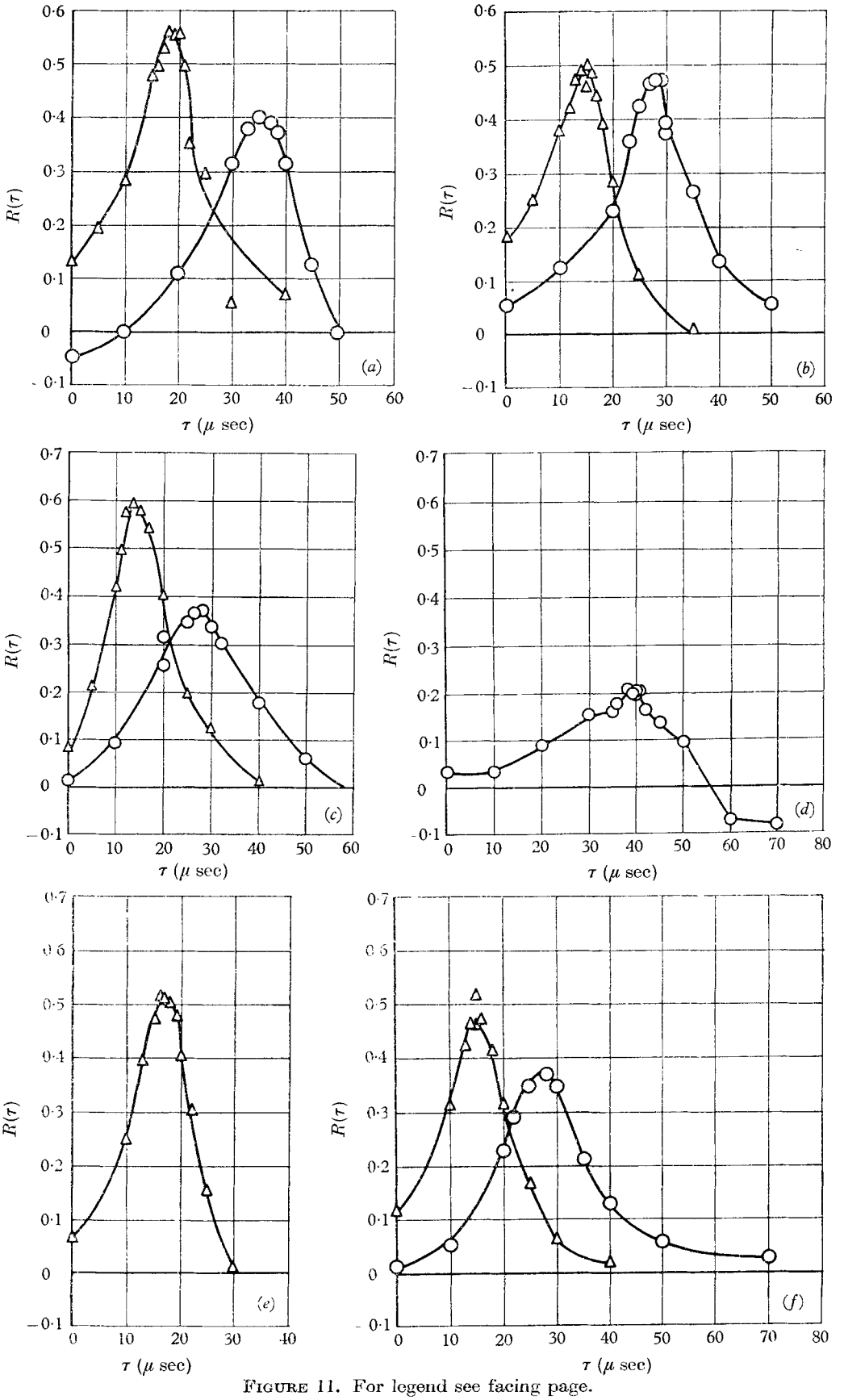

FIGURE 11. For legend see facing page.

Morkovin (1962) of the spectrum of the velocity fluctuations in a Mach number 1·76 boundary layer shows that the length scale of the velocity fluctuations here is about the same as for an incompressible boundary layer, i.e. $L_p/\delta \approx 0{\cdot}4$. Therefore, even at $M = 1{\cdot}33$, the pressure field has a significantly smaller length scale than the velocity field.

Figure 10 shows measurements of hot-wire spectra obtained in the side-wall boundary layers. The wire operating conditions were such that the primary sensitivity was to temperature fluctuations. In agreement with Morkovin's results, the length scales of the temperature fluctuations are 0·1 of the boundary-layer thickness. The average pressure spectrum for $M > 2$ is sketched in the figure to show how the pressure spectra compare with the temperature spectra.

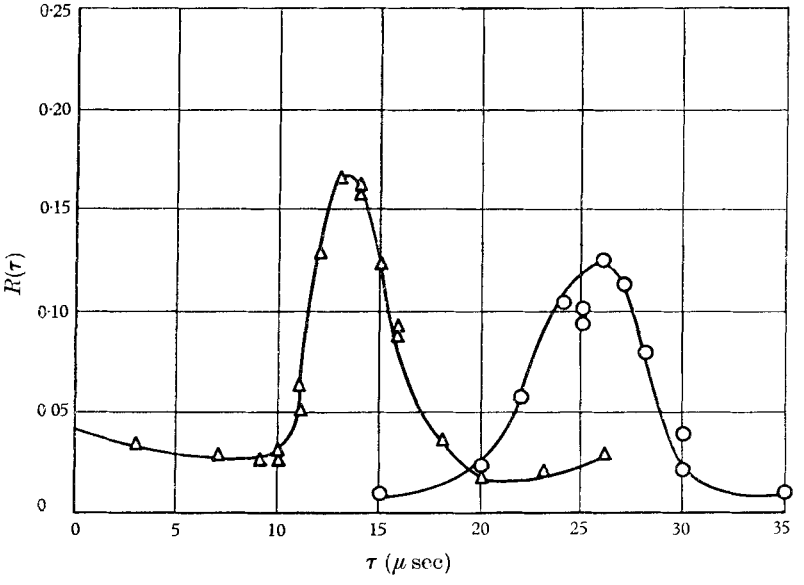

FIGURE 12. Measured space-time correlations on the flat plate. $M = 3{\cdot}25$, $U_\infty = 24{,}800$ in./sec, $Re_\theta = 0{\cdot}32 \times 10^4$, $d = 0{\cdot}03$ in., $\delta = 0{\cdot}25$ in.; △, $\Delta x = 0{\cdot}25$ in.; ○, $\Delta x = 0{\cdot}50$ in.

Also shown is the velocity spectrum obtained by Klebanoff (1954) in an incompressible boundary layer. The results of Morkovin indicate that the compressible velocity spectra are about the same as the incompressible spectrum measured by Klebanoff.

Correlations

The space-time correlations considered here are

$$\langle p^2 \rangle R(\Delta x, \tau) = \langle p(x, y, t)\, p(x + \Delta x, y, t + \tau) \rangle$$

where x is the streamline direction. As is known from subsonic results (Willmarth), the shape of the correlation curve obtained for a fixed longitudinal spacing of the transducers and a variable time delay between the two signals displays a maximum for a particular value of the time delay, $\tau_{\max}$. A velocity, the so-called convection velocity, can be constructed by dividing the spacing

Δx by the time $\tau_{\max}$, and this velocity can be interpreted as the speed at which the pressure field is moving along the wall. The correlation function can be characterized by this speed and by the rate at which the value of $R(\xi, \tau)$ decreases for increased spacing of the transducers. Only the first variation is included in the length-correction calculations. Typical measured correlation functions are shown in figures 11 and 12. The results in figure 11 were obtained on the side-wall with the electronic correlator; the results in figure 12 were obtained on the flat plate using the lumped circuit delay line.

The convection speed $\Delta x/\tau_{\max}$ obtained from these data is shown in figure 13 as a function of Mach number. The speeds shown were computed only from side-wall data, obtained with the electronic correlator. Willmarth's subsonic data

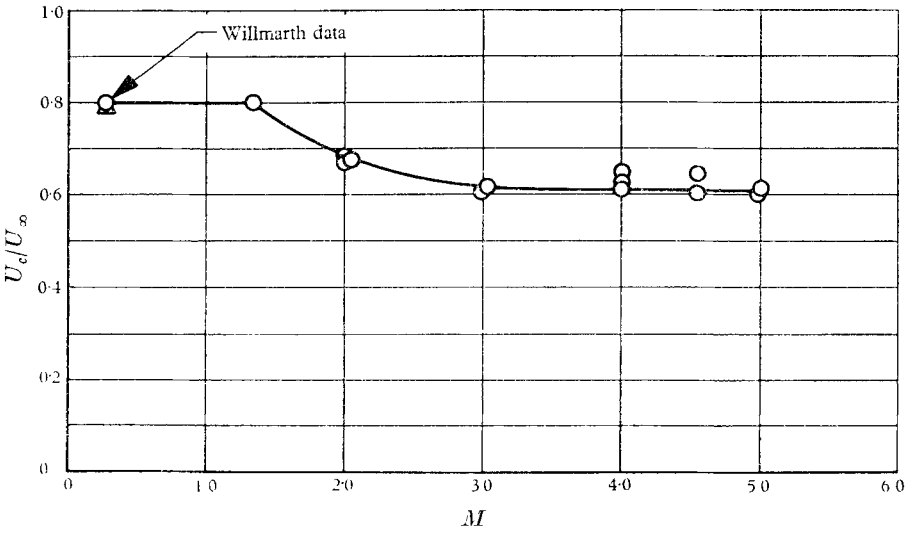

FIGURE 13. The convection speed ratio.

are also shown. At $M = 2{\cdot}00$, the tunnel Reynolds number was changed by a factor of 10, and it was found that there was no measurable change in the correlation shape or in the convection speed over this range of Reynolds number.

The rate of decay of the peak values of the correlation coefficient for various Mach numbers is illustrated in figure 14(*a*), where the peak value is plotted *vs* the non-dimensional distance $\Delta x/\delta$. The absolute value of the correlation was measured by extending the time delay in the measurement until the correlation had dropped to a constant value, which in the absence of extraneous signals should have been zero. The peak value was assumed to be the difference between this level value and the measured peak.

The data shown for $\Delta x/\delta < 0{\cdot}6$ were obtained on the side-wall and for $\Delta x/\delta > 0{\cdot}6$ on the flat plate. Assuming that these data are comparable, curves of the maximum value as a function of distance are sketched in. The general shape of the curve is a sharp drop from the value 1 at $\Delta x = 0$ to about the value of $\frac{1}{2}$ at $\Delta x/\delta = 0{\cdot}2$, and then a more gentle variation for larger Δx. There is no outstanding effect of Mach number on the decay of the peak value, but careful examination

of the data seems to indicate a trend for the peak to fall more rapidly for smaller M. The peak values are plotted against $\Delta x/\delta^*$ in figure 14(*b*), were δ^* is the boundary-layer displacement thickness, which gives a little better collapse of the data for large M_∞ and Δx.

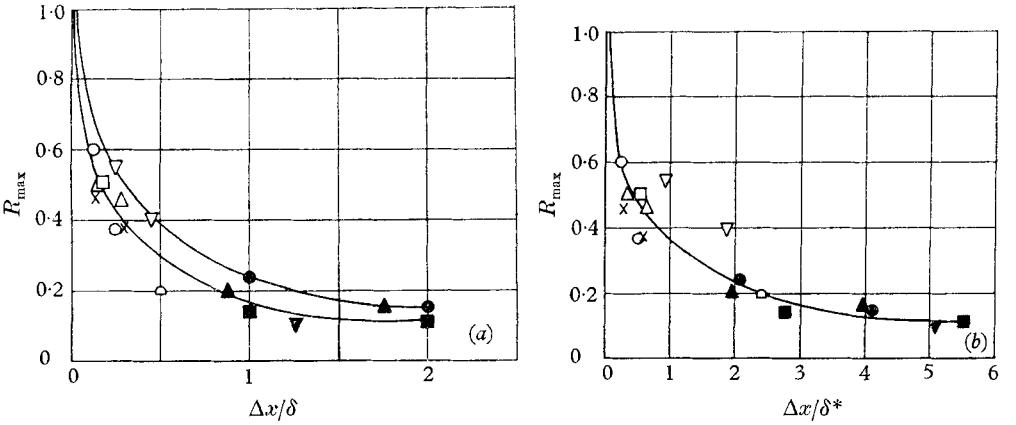

FIGURE 14. Peak values of the correlation for various transducer spacings. ○, M = 5·00; △, M = 4·00; □, M = 3·0; ▽, M = 2·0; ×, M = 4·54; ⌓, 1·33. Solid symbols, flat plate data with lumped delay line.

Fluctuation levels

The determination of the fluctuation levels from the calibrated transducers requires the integration of the measured power spectra. This method is more desirable than the direct measurement of the mean-square voltage because energy associated with the transducer can be removed from the spectra, and a length correction can be applied to the spectra before integration to obtain a more accurate result.

In the equilibrium flat-plate boundary layers considered here, it is to be expected that the R.M.S. pressure fluctuation level divided by some characteristic pressure, such as the local free-stream dynamic pressure, should be a function only of the Mach number and a Reynolds number based on the local boundary-layer thickness. The Reynolds number variation of $\langle p^2 \rangle$ was investigated primarily on the flat plate, since the Reynolds number could be varied over a wide range thereby varying not only the tunnel conditions but also the location of the transducer on the plate.

When the mean pressure level is varied and the spectra are measured at one point, the shape and magnitude of the measured spectra change for two reasons. As the mean pressure is increased, the boundary layer becomes thinner, and consequently the energy associated with the large eddies spreads to higher frequencies. At the same time, the spectra are affected by the change in Reynolds number Re. The spread of the energy to higher frequencies changes the length correction for different Reynolds numbers, and in order to obtain the pure Reynolds-number effect, the length correction must be introduced.

The data obtained from the flat plate were corrected, as explained earlier. The size of the correction on the measured $\langle e^2 \rangle$ was as large as a factor of 2 in

some cases. The corrected data are shown in figure 15. Owing to the size of the length correction, the relative values of $\tilde{p} = \langle p^2 \rangle^{\frac{1}{2}}$ obtained from different spectra at the same Mach number but at different Reynolds numbers are more accurate than the absolute values. Therefore, only the values of

$$\tilde{p}/\tilde{p}(Re_{\delta *} = U_\infty \delta^*/\nu_\infty = 10^4)$$

are shown in figure 15. The absolute level was determined from the side-wall measurements, where the corrections were much smaller. It is seen that for all

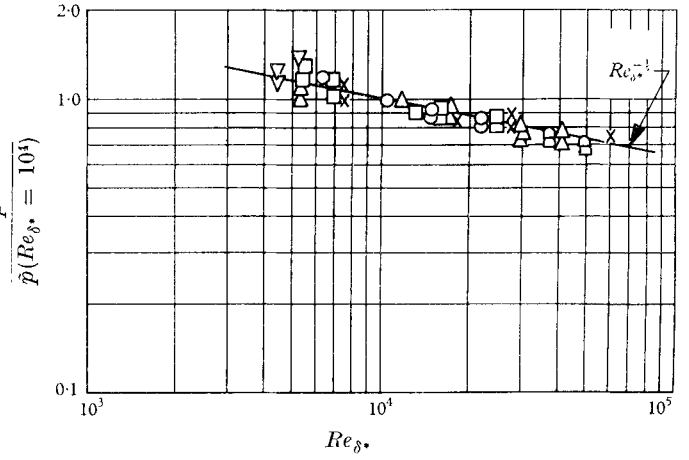

FIGURE 15. Corrected flat-plate data: $\tilde{p}$ variation with Reynolds number. ▽, △, $M = 2{\cdot}0$; □, $M = 3{\cdot}25$; ×, $M = 3{\cdot}99$; ⌓, $M = 4{\cdot}76$; ○, $M = 5{\cdot}00$.

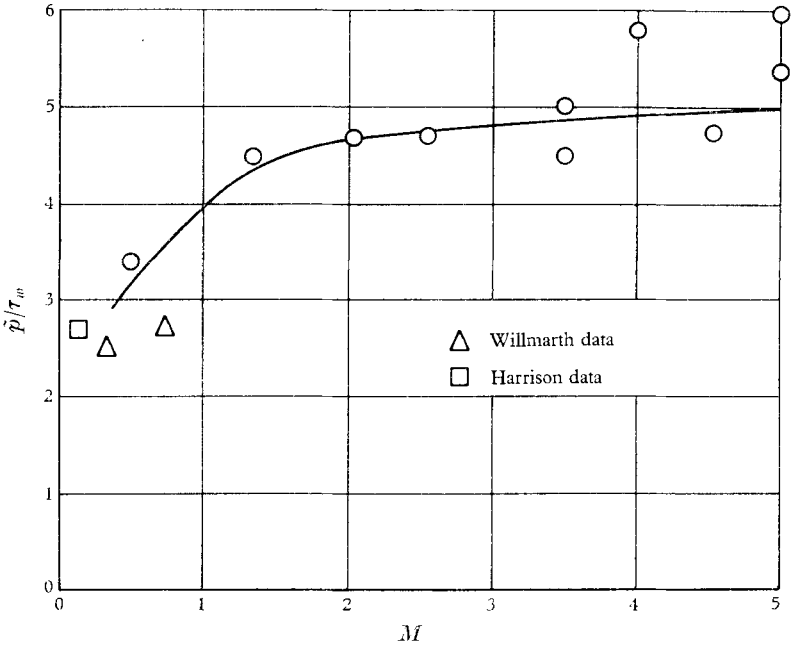

FIGURE 16. Pressure fluctuation levels.

Mach numbers the corrected levels of $\tilde{p}/q$ have a variation with Reynolds number close to $\tilde{p}/q \sim Re_\delta^{-\frac{1}{4}}$, where $Re_\delta = U_\infty \delta/\nu_\infty$ and $q = \frac{1}{2}\rho_\infty U_\infty^2$, which suggests that if the skin friction were used as the characteristic pressure, the effect of Reynolds number on $\tilde{p}$ would be accounted for.

The pressure fluctuation levels obtained on the side-wall are shown in figure 16, where τ_ω, the mean skin friction at the wall, is used to remove the Reynolds number influence. The magnitude of $\tilde{p}/\tau_\omega$ changes only little with Mach number above $M_\infty > 2$; τ_ω was computed using the compilation of Van Driest (1956).

The subsonic results of Willmarth and Harrison are plotted on the same scale and are seen to be significantly lower than the supersonic results. In order to see if our technique gave the same results at low speeds, one measurement was made on the flat plate with the tunnel choked near the diffuser so that there was subsonic flow over the flat plate. The sharp leading edge had to be modified with a wood filler to prevent the flow from separating. One pressure fluctuation measurement, also plotted on the curve, was obtained at $M_\infty = 0{\cdot}6$. This point is higher than Willmarth's data, but does indicate a trend of smaller $\tau/\tilde{p}_\omega$ at lower speeds when compared to the supersonic data.

7. Discussion

The data that exist concerning the structure of the turbulence in supersonic boundary layers show that the velocity field is not strongly influenced by Mach-number effects, at least in the outer regions of the boundary layer (Morkovin 1962). The measurements reported here of the wall pressure field of a supersonic boundary layer show that the root-mean-square level of the pressure divided by the local shear is higher than the subsonic value but remains reasonably constant above Mach number 2. The scale of the pressure fluctuations, however, changes in relation to the scale of the velocity field. The length scale for the pressure field above Mach number 2 is proportional to the momentum thickness of the boundary layer, but it is not clear what physical significance can be ascribed to this fact. The momentum thickness is a defined quantity whose gradient is related to the local skin friction but whose numerical value is not meaningful with respect to the dynamics of the turbulence.

A possible explanation for the change in the scale of the pressure field in contrast to the velocity field is that the existence of regions of relatively supersonic mean flow strongly affects the structure of the pressure field within the boundary layer even though the distribution and strengths of the pressure sources (velocity fluctuations) are only weakly dependent on the Mach number. It is reasonable to expect this effect of compressibility to increase the wall pressure produced by eddies near the wall and to decrease the wall pressure associated with the larger eddies in the outer regions of the boundary layer as the Mach number is increased. Such a trend would be consistent with the experimental results in that both the scale and the convection velocity of the wall pressures would be decreased as the Mach number is increased.

The maximum mean velocity of an eddy whose influence is subsonic at the wall is computed in the Appendix. An adiabatic boundary layer is assumed. If this velocity is converted to distance from the wall, z, assuming a $\frac{1}{7}$-power velocity

profile, z/δ for such an eddy varies from 0·39 at $M = 1{\cdot}33$ to 0·06 at $M = 2{\cdot}00$. Therefore, the range of mean velocities where an eddy has a subsonic influence on the wall decreases rapidly as the Mach number increases, and already at $M = 2{\cdot}00$ the corresponding region of flow is only a small fraction of the boundary-layer thickness.

The space-time correlation along the stream direction changes rapidly in magnitude; in fact, it has fallen to half its initial peak value within $\frac{1}{5}$ of a boundary-layer thickness. This rapid fall-off indicates that the eddies contributing to the pressure at the wall have widely differing velocities or that the eddies themselves vary rapidly in a co-ordinate system fixed to their centres. Since measurements of Favre, Gaviglio & Dumas (1958) of the space-time correlation of the velocity fluctuations in a subsonic boundary layer have shown that the turbulence pattern—at least away from the wall—moves with the local velocity and does not vary rapidly in distances comparable to the boundary-layer thickness, it is probable that the pressure correlations on the wall—and perhaps also the velocity correlations near the wall—decrease to small values within a short distance because of the wide range of mean velocities of the large eddies that add up to give the wall effects.

A useful theory for the pressure fluctuations would have to predict not only the fluctuation levels but also the properties of the correlation function. If the ideas expressed above are correct, this would imply that some knowledge of the relationship of the large-eddy motion in the turbulence to the pressure field at the wall would be required, as well as a knowledge of the essential properties of the turbulent eddies. For example, what is the distribution of the location of the centres of the eddies, i.e. that part of the organized eddy motion that moves with the local mean speed? The currently available theories bypass such problems with *ad hoc* assumptions, and important information is lost.

Most of the current information on the properties of turbulent boundary layers has been obtained with a hot-wire anemometer. Therefore, it is of interest to examine the way in which the results of this work can affect the interpretation of a hot-wire signal obtained from a supersonic boundary layer. It has been shown (Kistler 1959) that the output of a hot wire in a supersonic boundary layer can be decomposed into a contribution by a velocity ($\tilde{U}$) and by a temperature ($\tilde{T}$) or density ($\tilde{\rho}$) fluctuation if one can assume that the pressure ($\tilde{p}$) fluctuation level is much smaller than the levels of the other fluctuation; i.e. if

$$\tilde{p}/\overline{p} < \tilde{\rho}/\overline{\rho}, \quad \tilde{T}/\overline{T}, \quad \tilde{U}/\overline{U},$$

where $\overline{p}$, $\overline{\rho}$, $\overline{T}$ and $\overline{U}$ represent mean values, and $\tilde{p}$, $\tilde{T}$, $\tilde{\rho}$ and $\tilde{U}$ represent R.M.S. fluctuations. Since the experiments reported here show for $M > 2$, $\tilde{p}/\tau_w \approx 5$ at the wall, we can write

$$\tilde{p}/\tau_w = \tilde{p}/C_f q = \tilde{p}/\tfrac{1}{2}C_f \gamma_p M^2 = 5,$$

where $C_f = \tau_w/q$ is the local skin-friction coefficient and γ the ratio of the specific heats. Therefore

$$\tilde{p}/\overline{p} \approx 2{\cdot}5\gamma M^2 C_f.$$

A typical value for C_f is 10^{-3} and $\gamma = 1{\cdot}4$, so that $\tilde{p}/\overline{p} \approx 3{\cdot}5 \times 10^{-3} M^2$. For $M_\infty = 5$, $\tilde{p}/\overline{p} \approx 8{\cdot}75 \times 10^{-2} = 8{\cdot}75\,\%$. This value is comparable to the velocity

fluctuation level in a boundary layer, so it appears that for M in the neighbourhood of 5 or larger the simple constant-pressure interpretation of the data is no longer possible. Any results obtained for these large Mach numbers will have to incorporate some knowledge of the pressure field and its relation to the turbulent velocity field.

8. Conclusion

Measurements of the wall pressure field associated with a supersonic turbulent boundary layer have been obtained for flow Mach numbers up to 5·0. The major effect of increasing the Mach number is to decrease the length scale of the pressure field. The integral scale of the wall-pressure fluctuations changes from 16 % of the boundary-layer thickness at $M = 1{\cdot}33$ to 0·06 % at $M = 4{\cdot}54$. The R.M.S. level of the pressures is proportional to the local mean shear for all Mach numbers, and the proportionality constant changes from about 3 for subsonic boundary layers to about 5 for Mach numbers greater than 2.

The convection speed characterizing the pressure correlation on the wall decreases with increasing Mach number, and within the accuracy of measurement is independent of Reynolds number. The maximum value of the pressure correlation falls off rapidly with increased spatial separation of the measuring points, and the peak is down to a value of $\frac{1}{2}$ at about $\Delta x = 0{\cdot}2\delta$. The rapid decrease of the correlation implies that the eddies contributing to the wall pressure move with a large range in speeds, so that the convection speed represents some weighted average of these speeds.

The main limitation to the data reported here lies in the uncertain nature of the length correction, but this limit can only be removed if a better grasp of the structure of the pressure field throughout the boundary layer is obtained.

Appendix

Maximum speed of an eddy with subsonic influence at the wall

The data presented in this report make it clear that the convection speed represents not some unique velocity for an eddy pattern, but instead is the weighted average over many eddy velocities. Still, it is of some interest to examine the relationship of this speed to the various sonic velocities of importance in a boundary layer. Here we refer to the sonic lines relative to an eddy moving with some velocity U_0 with respect to the wall, i.e. the boundary between the region where the eddy has a subsonic influence and the region where the eddy has a supersonic influence. Such a sonic line satisfies $U_1 - U_0 = a_1$, where U_1 is the local mean velocity on the sonic line and a_1 is the local sonic velocity. If we assume that we are dealing with a perfect-gas flow with constant specific heats, then for an adiabatic boundary layer with an effective Prandtl number of one the energy equation is $C_p T + \frac{1}{2}U^2 = C_p T_0$ (C_p is the specific heat at constant pressure). It follows that the condition relating U_1 and U_0 is

$$\left(\frac{U_1}{U_\infty}\right)^2 - \frac{4}{\gamma+1}\frac{U_0 U_1}{U_\infty^2} + \frac{2}{\gamma+1}\left(\frac{U_0}{U_\infty}\right)^2 - \frac{\gamma-1}{\gamma+1} - \frac{2}{\gamma+1}\frac{1}{M_\infty^2} = 0,$$

where U_∞ and M_∞ are the free-stream velocity and Mach number, respectively.

Of interest is the eddy velocity U_0 where the wall is a sonic line, i.e. $U_1/U_\infty = 0$, or the maximum speed at which the eddy has a subsonic influence at the wall. We obtain

$$(U_0/U_\infty)^2 = 0{\cdot}2 + 1/M_\infty^2$$

if $\gamma = 1{\cdot}4$. For an eddy moving with this velocity, the region of subsonic influence extends away from the wall to a region of velocity

$$(U_1/U_\infty)^2 = 2{\cdot}78(0{\cdot}2 + 1/M_\infty^2).$$

These two curves are plotted in figure 17, along with the measured values of the convection speed. Of interest is the fact that even at $M = \infty$, under the condition postulated, an eddy with a subsonic influence at the wall has a subsonic influence in the boundary layer out to the point where $U_1/U_\infty = 0{\cdot}75$, a finite fraction of the boundary-layer thickness. This serves to illustrate the fact that some care has to be taken in making assumptions with respect to the limit of $M \to \infty$.

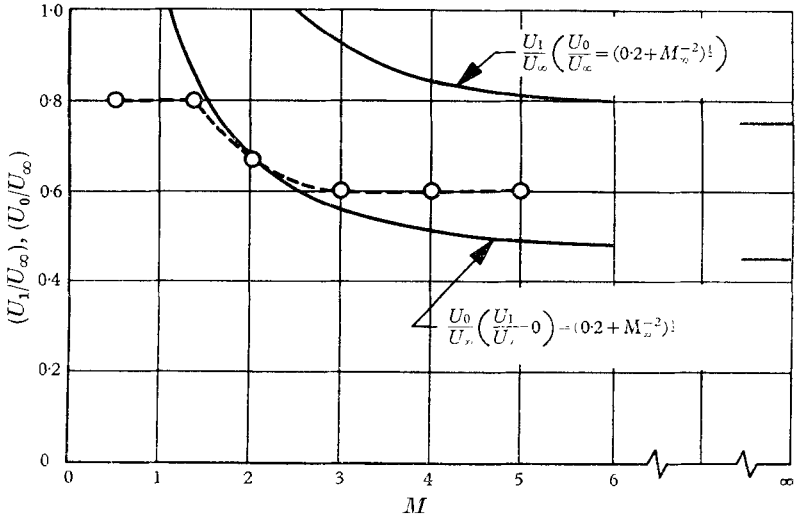

FIGURE 17. Subsonic region associated with eddy with subsonic influence at wall.

Phillips (1960) assumed that the width of the subsonic region, in an analogous problem, shrinks to zero essentially as $1/M$ as $M \to \infty$. This implies a similarity of the Mach number field as $M \to \infty$, which is not true if T_0 = constant is a constraint.

The experimental values for the convection speed are approximately equal to the eddy velocity that has a sonic influence on the wall up to $M = 3$. Above $M = 3$, the convection speed levels off at $U_c/U_\infty = 0{\cdot}6$, and the eddies primarily responsible for the wall pressure move supersonically with respect to the wall.

The work reported here was done at the California Institute of Technology Jet Propulsion Laboratory under NASA Contract NAS 7–100.

REFERENCES

CHEN, W. 1961 Aeronautical Engineering Thesis, California Institute of Technology.

CORCOS, G., CUTHBERT, J. W. & VON WINKLE, W. A. 1959 Institute of Engineering Research, University of California, Berkeley, Series 82, Issue 12.

FAVRE, A. J., GAVIGLIO, J. J. & DUMAS, R. J. 1958 *J. Fluid Mech.* **3**, 344–56.

HARRISON, M. 1958 David Taylor Model Basin, Maryland, *Report* 1260.

KISTLER, A. L. 1959 *Phys. Fluids*, **2**, 290–6.

KLEBANOFF, P. 1954 Washington, D.C., *NACA Technical Note* 3178.

KRAICHNAN, R. H. 1957 *J. Acoust. Soc. Amer.* **29**, 65–80.

LAUFER, J. 1961 *J. Aerospace Sci.* **28**, 685–92.

LILLEY, G. M. & HODGSON, T. H. 1960 On surface pressure fluctuations in turbulent boundary layers. *AGARD Report* 276.

MORKOVIN, M. V. 1962 Effects of compressibility on turbulent flows. *Méchanique de la Turbulence*. CNRS, Paris, France.

PHILLIPS, O. M. 1960 *J. Fluid Mech.* **9**, 1–28.

VAN DRIEST, E. R. 1956 The problem of aerodynamic heating. *Aero. Eng. Rev.* **15**, 26–41.

WILLMARTH, W. W. 1958 *Rev. Sci. Instr.* **29**, 218–22.

WILLMARTH, W. W. 1959 National Aeronautics and Space Administration, Washington, D.C., *Memorandum* 3-17-59W.

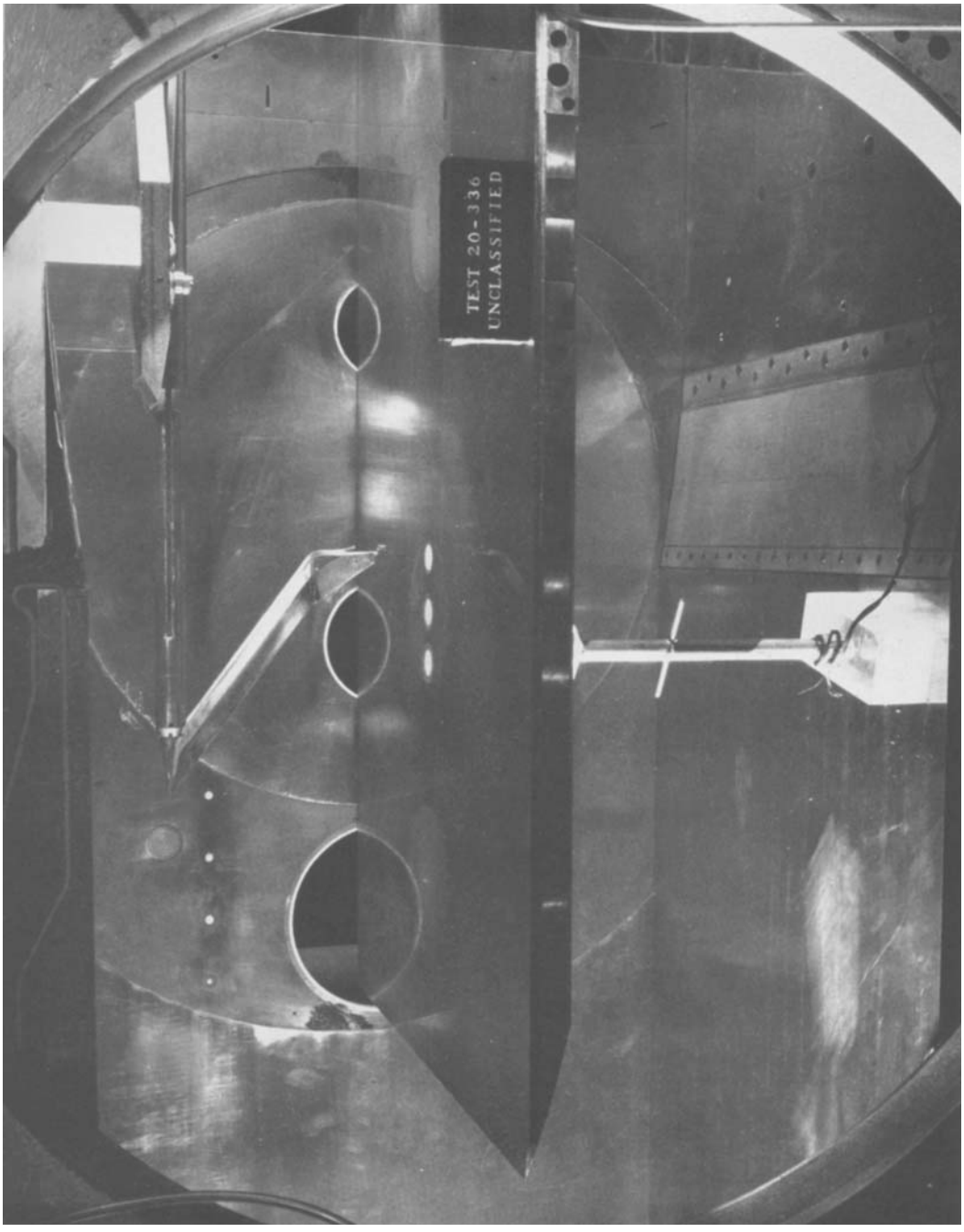

FIGURE 1. Transducer installation on flat plate.

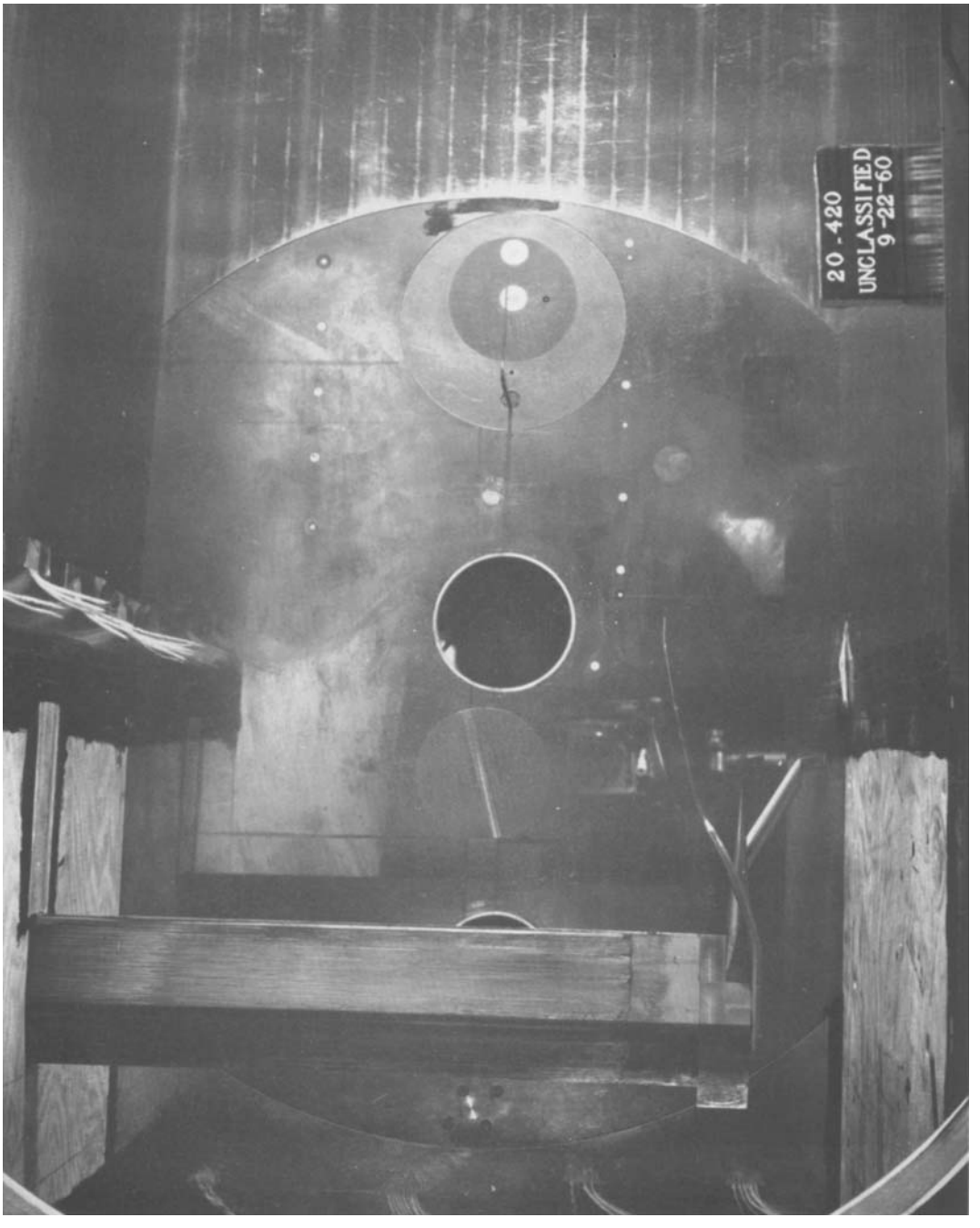

FIGURE 2. Transducer installation on tunnel side-wall.

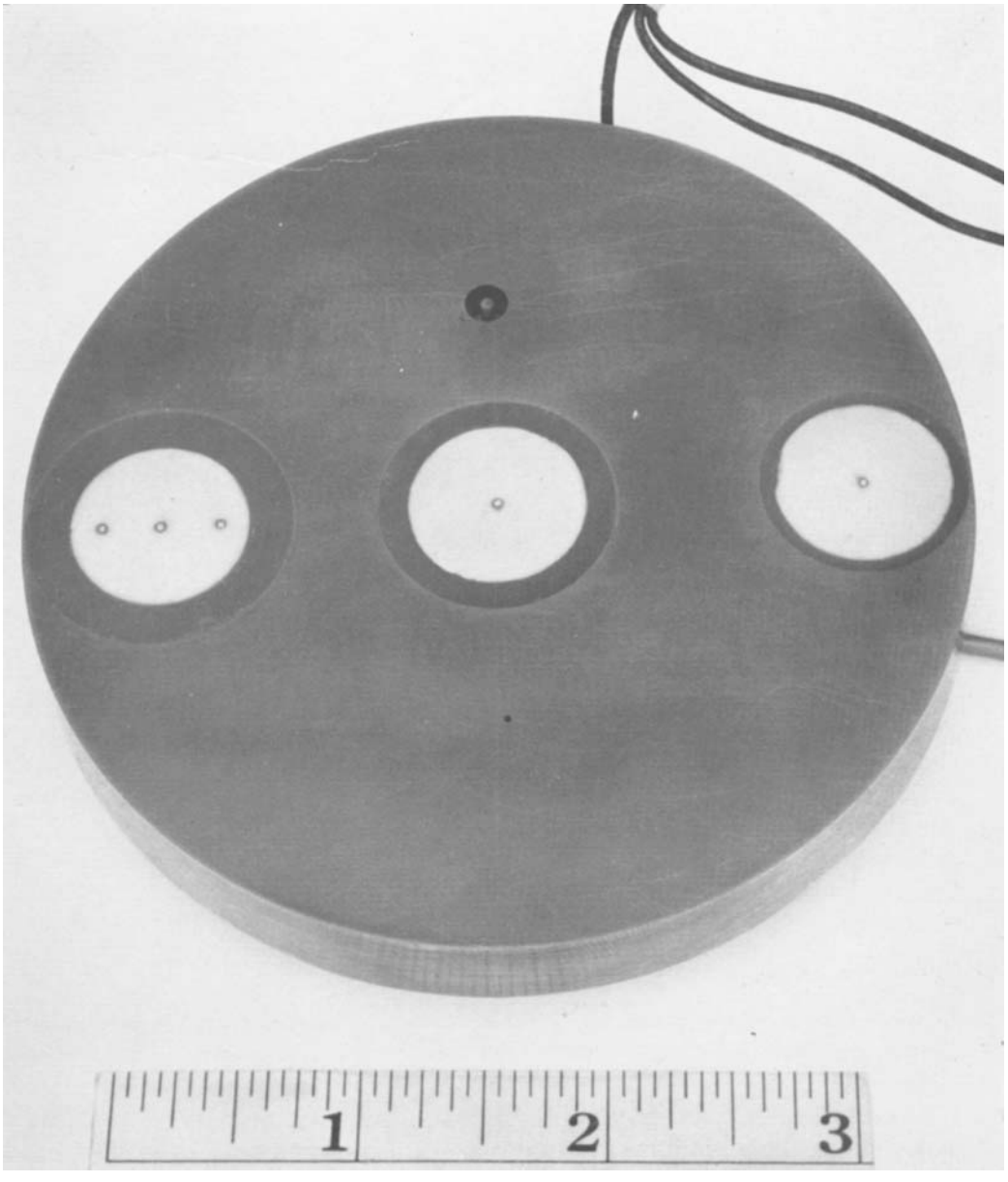

FIGURE 4. Photograph of transducers installed in mounting disk.